

---

# An adaptive ANOVA stochastic Galerkin method for partial differential equations with random inputs

Guanjie Wang · Smita Sahu · Qifeng Liao

Received: date / Accepted: date

**Abstract** It is known that standard stochastic Galerkin methods encounter challenges when solving partial differential equations with high dimensional random inputs, which are typically caused by the large number of stochastic basis functions required. It becomes crucial to properly choose effective basis functions, such that the dimension of the stochastic approximation space can be reduced. In this work, we focus on the stochastic Galerkin approximation associated with generalized polynomial chaos (gPC), and explore the gPC expansion based on the analysis of variance (ANOVA) decomposition. A concise form of the gPC expansion is presented for each component function of the ANOVA expansion, and an adaptive ANOVA procedure is proposed to construct the overall stochastic Galerkin system. Numerical results demonstrate the efficiency of our proposed adaptive ANOVA stochastic Galerkin method.

## 1 Introduction

Over the past few decades, there has been a significant increase in efforts to develop efficient uncertainty quantification approaches for solving partial differential equations (PDEs) with random inputs. Typically, these random inputs arise from a lack of precise measurements or a limited understanding of realistic model parameters, such as permeability coefficients in diffusion problems and refraction coefficients in acoustic problems [24, 7, 8].

Designing a surrogate model or calculating statistics, such as mean and variance of the stochastic solution, for partial differential equations (PDEs) with random inputs, especially high dimensional ones, is of great interest. To achieve this, extensive efforts have been made. The Monte Carlo method

---

Guanjie Wang  
School of Statistics and Mathematics, Shanghai Lixin University of Accounting and Finance, Shanghai, China.  
E-mail: guanjie@lixin.edu.cn

Smita Sahu  
School of Mathematics and Physics, University of Portsmouth, Lion Terrace, PO1 3HF, UK.  
The Faraday Institution, Quad One, Becquerel Avenue, Harwell Campus, Didcot, OX11 0RA, UK.  
E-mail: smita.sahu@port.ac.uk

Qifeng Liao  
School of Information Science and Technology, ShanghaiTech University, Shanghai, China.  
E-mail: liaoqf@shanghaitech.edu.cn

(MCM) and its variants are among the simplest methods for computing the mean and variance [5, 9]. In MCM, numerous sample points of the random inputs are generated based on their probability density functions. For each sample point, the corresponding deterministic problem can be solved using existing numerical methods. The statistics of the stochastic solution can then be estimated by aggregating the results of these deterministic solutions. While MCM is easy to implement, it converges slowly and typically requires a large number of sample points. Additionally, it does not provide a surrogate model directly, which can be crucial in certain scenarios.

To enhance efficiency, the stochastic collocation method (SCM) and the stochastic Galerkin method (SGM) have been developed. Both SCM and SGM are more efficient than MCM for solving partial differential equations (PDEs) with moderate dimensional random inputs [23, 24, 25, 26]. However, these methods face challenges in addressing high dimensional problems, as the number of collocation points required by SCM and the number of unknowns in SGM increase rapidly with an increasing number of random variables, a well-established phenomenon referred to as the curse of dimensionality.

To address the challenges posed by high dimensional problems, some novelty techniques have been developed and implemented. For example, the adaptive sparse grids [1], multi-element generalized polynomial chaos [20], and anchored ANOVA methods (i.e. cut-HDMR) [14, 27]. In particular, the anchored ANOVA method has been extensively employed in various research studies (see for instance [18, 10, 17, 12]). It is shown that a bad choice of the anchor point can lead to an unacceptable approximation error [21, 16], the literature [18] analyzes the reason of this sensitivity to anchor point, and proposes to use the covariance decomposition capable of evaluating very accurately the output variance of multivariate function in the framework of anchored ANOVA. A disadvantage of this anchor based global method is also that a surrogate model cannot be built in a straightforward way [19].

In this paper, we investigate the generalized polynomial chaos (gPC) expansion of component functions for the ANOVA decomposition, and present a concise form of the gPC expansion for each component function. With this foundation, we propose an adaptive ANOVA stochastic Galerkin method for solving partial differential equations with random inputs. The proposed method adaptively selects the effective gPC basis functions in the stochastic space, reducing the dimension of the stochastic approximation space significantly, and leveraging the orthonormality of the gPC basis to facilitate the computation of the variance of each term in the ANOVA decomposition. Additionally, the proposed method provides a straightforward approach to building a surrogate model. We conduct numerical simulations and present the results to demonstrate the effectiveness and efficiency of our proposed method.

An outline of the paper is as follows. We present our problem setting in the next section. In Section 3, we review the stochastic Galerkin method and the ANOVA decomposition for partial differential equations with random inputs. Our main theoretical results and the adaptive ANOVA stochastic Galerkin method are presented in Section 4. Numerical results are discussed in Section 5. Section 6 concludes the paper.

## 2 Problem setting

Let  $D \subseteq \mathbb{R}^d$  ( $d = 2, 3$ ) denote a physical domain that is bounded, connected, with a polygonal boundary  $\partial D$ , and where  $\mathbf{x} \in \mathbb{R}^d$  denote a physical variable. Let  $\boldsymbol{\mu} = (\mu_1, \dots, \mu_N)$  be a random vector of dimension of  $N$ , where the image of  $\mu_i$  is denoted by  $\Gamma_i$ , and the probability density

function of  $\mu_i$  is denoted by  $\rho_i(\mu_i)$ . We further assume that the components of  $\boldsymbol{\mu}$ , i.e.,  $\mu_1, \dots, \mu_N$  are mutually independent, then the image of  $\boldsymbol{\mu}$  is given by  $\Gamma = \Gamma_1 \times \dots \times \Gamma_N$ , and the probability density function of  $\boldsymbol{\mu}$  is given by  $\rho(\boldsymbol{\mu}) = \prod_{i=1}^N \rho_i(\mu_i)$ . In this work, we focus on the partial differential equations (PDEs) with random inputs, that is

$$\begin{cases} \mathfrak{L}(\boldsymbol{x}, \boldsymbol{\mu}, u(\boldsymbol{x}, \boldsymbol{\mu})) = f(\boldsymbol{x}) & \forall (\boldsymbol{x}, \boldsymbol{\mu}) \in D \times \Gamma, \\ \mathfrak{b}(\boldsymbol{x}, \boldsymbol{\mu}, u(\boldsymbol{x}, \boldsymbol{\mu})) = q(\boldsymbol{x}) & \forall (\boldsymbol{x}, \boldsymbol{\mu}) \in \partial D \times \Gamma, \end{cases} \quad (2.1)$$

where  $\mathfrak{L}$  is a linear partial differential operator with respect to physical variables, and  $\mathfrak{b}$  is a boundary operator. Both operators may have random coefficients. The source function is denoted by  $f(\boldsymbol{x})$ , and  $q(\boldsymbol{x})$  specifies the boundary conditions. Additionally, we assume that  $\mathfrak{L}$  and  $\mathfrak{b}$  are affinely dependent on the random inputs. Specifically, we have

$$\mathfrak{L}(\boldsymbol{x}, \boldsymbol{\mu}, u(\boldsymbol{x}, \boldsymbol{\mu})) = \sum_{i=1}^K \Theta_{\mathfrak{L}}^{(i)}(\boldsymbol{\mu}) \mathfrak{L}_i(\boldsymbol{x}, u(\boldsymbol{x}, \boldsymbol{\mu})), \quad (2.2)$$

$$\mathfrak{b}(\boldsymbol{x}, \boldsymbol{\mu}, u(\boldsymbol{x}, \boldsymbol{\mu})) = \sum_{i=1}^K \Theta_{\mathfrak{b}}^{(i)}(\boldsymbol{\mu}) \mathfrak{b}_i(\boldsymbol{x}, u(\boldsymbol{x}, \boldsymbol{\mu})), \quad (2.3)$$

where  $\{\mathfrak{L}_i\}_{i=1}^K$  are parameter-independent linear differential operators, and  $\{\mathfrak{b}_i\}_{i=1}^K$  are parameter-independent boundary operators. Both  $\Theta_{\mathfrak{L}}^{(i)}(\boldsymbol{\mu})$  and  $\Theta_{\mathfrak{b}}^{(i)}(\boldsymbol{\mu})$  take values in  $\mathbb{R}$  for  $i = 1, \dots, K$ .

It is of interest to design a surrogate model for the problem (2.1) or calculate statistics, such as mean and variance, of the stochastic solution  $u(\boldsymbol{x}, \boldsymbol{\mu})$ .

### 3 Stochastic Galerkin method and ANOVA decomposition

In this section, we shall introduce the stochastic Galerkin methods for solving problem (2.1), and subsequently, we shall revisit the ANOVA decomposition for multi-variable functions. For the sake of presentation simplicity, we shall consider problems that satisfy homogeneous Dirichlet boundary conditions. However, it is noteworthy that the approach we shall present can be readily extended to nonhomogeneous boundary conditions.

#### 3.1 Variational formulation

To introduce the variational form of (2.1), some notations are required. We first define the Hilbert spaces  $L^2(D)$  and  $L^2_{\rho}(\Gamma)$  via

$$\begin{aligned} L^2(D) &:= \left\{ v(\boldsymbol{x}) : D \rightarrow \mathbb{R} \mid \int_D v^2(\boldsymbol{x}) \, d\boldsymbol{x} < \infty \right\}, \\ L^2_{\rho}(\Gamma) &:= \left\{ g(\boldsymbol{\mu}) : \Gamma \rightarrow \mathbb{R} \mid \int_{\Gamma} \rho(\boldsymbol{\mu}) g^2(\boldsymbol{\mu}) \, d\boldsymbol{\mu} < \infty \right\}, \end{aligned}$$

which are equipped with the inner products

$$\begin{aligned} \langle v(\boldsymbol{x}), \hat{v}(\boldsymbol{x}) \rangle_{L^2} &:= \int_D v(\boldsymbol{x}) \hat{v}(\boldsymbol{x}) \, d\boldsymbol{x}, \\ \langle g(\boldsymbol{\mu}), \hat{g}(\boldsymbol{\mu}) \rangle_{L^2_{\rho}} &:= \int_{\Gamma} \rho(\boldsymbol{\mu}) g(\boldsymbol{\mu}) \hat{g}(\boldsymbol{\mu}) \, d\boldsymbol{\mu}. \end{aligned}$$

Following presentation from Babuška et al.[3], we define the tensor space of  $L^2(D)$  and  $L^2_\rho(\Gamma)$  as

$$L^2(D) \otimes L^2_\rho(\Gamma) := \left\{ w(\mathbf{x}, \boldsymbol{\mu}) \left| w(\mathbf{x}, \boldsymbol{\mu}) = \sum_{i=1}^n v_i(\mathbf{x}) g_i(\boldsymbol{\mu}), v_i(\mathbf{x}) \in L^2(D), g_i(\boldsymbol{\mu}) \in L^2_\rho(\Gamma), n \in \mathbb{N} \right. \right\},$$

which is equipped with the inner product

$$\langle w(\mathbf{x}, \boldsymbol{\mu}), \hat{w}(\mathbf{x}, \boldsymbol{\mu}) \rangle_{L^2 \otimes L^2_\rho} = \sum_{i,j} \langle v_i(\mathbf{x}), \hat{v}_j(\mathbf{x}) \rangle_{L^2} \cdot \langle g_i(\boldsymbol{\mu}), \hat{g}_j(\boldsymbol{\mu}) \rangle_{L^2_\rho}.$$

It is clear that the tensor space  $L^2(D) \otimes L^2_\rho(\Gamma)$  is equipped with the tensor inner product

$$\langle w(\mathbf{x}, \boldsymbol{\mu}), \hat{w}(\mathbf{x}, \boldsymbol{\mu}) \rangle_{L^2 \otimes L^2_\rho} = \int_\Gamma \int_D w(\mathbf{x}, \boldsymbol{\mu}) \hat{w}(\mathbf{x}, \boldsymbol{\mu}) \rho(\boldsymbol{\mu}) d\mathbf{x} d\boldsymbol{\mu}.$$

We next define the space

$$H_0^1(D) := \{v \in H^1(D) \mid v = 0 \text{ on } \partial D\},$$

where  $H^1(D)$  is the Sobolev space

$$H^1(D) := \{v \in L^2(D), \partial v / \partial x_i \in L^2(D), i = 1, \dots, d\}.$$

To this end, we define the solution and test function space

$$W := H_0^1(D) \otimes L^2_\rho(\Gamma) = \left\{ w(\mathbf{x}, \boldsymbol{\mu}) \in H_0^1(D) \otimes L^2_\rho(\Gamma) \left| \|w(\mathbf{x}, \boldsymbol{\mu})\|_\otimes < \infty \right. \right\},$$

where  $\|\cdot\|_\otimes$  is the norm induced by the inner product  $\langle \cdot, \cdot \rangle_\otimes$ . The variational form of (2.1) can be written as: find  $u$  in  $W = H_0^1(D) \otimes L^2_\rho(\Gamma)$  such that

$$\mathfrak{B}(u, w) = \mathfrak{F}(w), \quad \forall w \in W, \quad (3.1)$$

where

$$\mathfrak{B}(u, w) := \langle \mathfrak{L}(\mathbf{x}, \boldsymbol{\mu}, u(\mathbf{x}, \boldsymbol{\mu})), w(\mathbf{x}, \boldsymbol{\mu}) \rangle_{L^2 \otimes L^2_\rho}, \quad \mathfrak{F}(w) := \langle f(\mathbf{x}), w(\mathbf{x}, \boldsymbol{\mu}) \rangle_{L^2 \otimes L^2_\rho}.$$

Since  $\mathfrak{L}$  is affinely dependent on the parameter  $\boldsymbol{\mu} \in \Gamma$  (see (2.2)) then  $\mathfrak{B}$  has the following form

$$\mathfrak{B}(u, w) = \sum_{i=1}^K \mathfrak{B}_i(u, w), \quad (3.2)$$

where the component bilinear forms  $\mathfrak{B}_i(\cdot, \cdot)$  for  $i \in \mathbb{N}^+$  are defined as

$$\mathfrak{B}_i(u, w) := \left\langle \Theta_\Sigma^{(i)}(\boldsymbol{\mu}) \mathfrak{L}_i(\mathbf{x}, u(\mathbf{x}, \boldsymbol{\mu})), w(\mathbf{x}, \boldsymbol{\mu}) \right\rangle_{L^2 \otimes L^2_\rho}. \quad (3.3)$$

### 3.2 Discretization

A discrete version of (3.1) is obtained by introducing a finite dimensional subspace to approximate  $W$ . Specifically, we first denote the finite dimensional subspaces of the corresponding stochastic and physical spaces by

$$S_p = \text{span} \{\Phi_j(\boldsymbol{\mu})\}_{j=1}^{n_\mu} \subseteq L^2_\rho(\Gamma), \quad V_h = \text{span} \{v_s(\mathbf{x})\}_{s=1}^{n_x} \subseteq H_0^1(D),$$

where  $\Phi_j(\boldsymbol{\mu})$  and  $v_s(\mathbf{x})$  refer to basis functions. We next define a finite dimensional subspace of the overall solution (and test) function space  $W$  by

$$W_h^p := V_h \otimes S_p := \text{span} \{v(\mathbf{x})\Phi(\boldsymbol{\mu}) \mid v \in V_h, \Phi \in S_p\}.$$

The stochastic Galerkin method seeks an approximation  $u^{\text{ap}}(\mathbf{x}, \boldsymbol{\mu}) \in W_h^p$  such that

$$\mathfrak{B}(u^{\text{ap}}, w) = \mathfrak{F}(w), \quad \forall w \in W_h^p,$$

Suppose  $u^{\text{ap}}(\mathbf{x}, \boldsymbol{\mu})$  is defined as

$$u^{\text{ap}}(\mathbf{x}, \boldsymbol{\mu}) := \sum_{s=1}^{n_x} \sum_{j=1}^{n_\mu} u_{sj} \Phi_j(\boldsymbol{\mu}) v_s(\mathbf{x}). \quad (3.4)$$

Since  $\mathfrak{L}$  is affinely dependent on the random inputs (see (2.2)), we substitute (3.4) into (3.3) to obtain

$$\mathfrak{B}_i(u^{\text{ap}}(\mathbf{x}, \boldsymbol{\mu}), w) = \sum_{s=1}^{n_x} \sum_{j=1}^{n_\mu} u_{sj} \Phi_j(\boldsymbol{\mu}) \left\langle \Theta_{\mathfrak{L}}^{(i)}(\boldsymbol{\mu}) \mathfrak{L}_i v_s(\mathbf{x}), w(\mathbf{x}, \boldsymbol{\mu}) \right\rangle_{L^2 \otimes L^2_\rho}. \quad (3.5)$$

Combining (3.5) with (3.1)–(3.2), we obtain a linear system for the unknown coefficients  $u_{sj}$ :

$$\left( \sum_{i=1}^K \mathbf{G}_i \otimes \mathbf{A}_i \right) \bar{\mathbf{u}} = \mathbf{h} \otimes \mathbf{f}, \quad (3.6)$$

where  $\{\mathbf{G}_i\}_{i=1}^K$  are matrices of size  $n_\mu \times n_x$ , and  $\mathbf{h}$  is a column vector of length  $n_\mu$ . They are defined via

$$\mathbf{G}_i(j, k) = \langle \Theta_{\mathfrak{L}}^{(i)}(\boldsymbol{\mu}) \Phi_j(\boldsymbol{\mu}), \Phi_k(\boldsymbol{\mu}) \rangle_{L^2_\rho}, \quad \mathbf{h}(i) = \langle \Phi_i(\boldsymbol{\mu}), 1 \rangle_{L^2_\rho}. \quad (3.7)$$

The matrices  $\mathbf{A}_i$  and the vector  $\mathbf{f}$  in (3.6) are defined through

$$\mathbf{A}_i(s, t) = \langle \mathfrak{L}_i v_s, v_t \rangle_{L^2}, \quad \mathbf{f}(s) = \langle \mathbf{f}, v_s \rangle_{L^2}, \quad (3.8)$$

where  $s = 1, \dots, n_x$  and  $t = 1, \dots, n_x$ . The vector  $\bar{\mathbf{u}}$  in (3.6) is a column vector of length  $n_x \times n_\mu$ , and is defined by

$$\bar{\mathbf{u}} = \begin{bmatrix} \mathbf{u}_1 \\ \vdots \\ \mathbf{u}_{n_\mu} \end{bmatrix}, \quad \text{where } \mathbf{u}_j = \begin{bmatrix} u_{1j} \\ \vdots \\ u_{n_x j} \end{bmatrix}, \quad j = 1, \dots, n_\mu.$$

### 3.3 ANOVA decomposition

We define some notations before introducing the ANOVA decomposition. Let  $\mathbb{T} = \{t_1, \dots, t_{|\mathbb{T}|}\}$  be a subset of  $\mathbb{U} = \{1, \dots, N\}$ , where  $|\mathbb{T}|$  is the cardinality of  $\mathbb{T}$ . For special case where  $\mathbb{T} = \emptyset$ , we set  $|\mathbb{T}|$  to 0. Otherwise, we assume that  $t_1 < t_2 < \dots < t_{|\mathbb{T}|}$ . In addition, for  $\mathbb{T} \neq \emptyset$ , let  $\boldsymbol{\mu}_{\mathbb{T}}$  denote the  $|\mathbb{T}|$ -vector that contains the components of the vector  $\boldsymbol{\mu}$  indexed by  $\mathbb{T}$ , i.e.,  $\boldsymbol{\mu}_{\mathbb{T}} = (\mu_{t_1}, \dots, \mu_{t_{|\mathbb{T}|}})$ . For a given cardinality  $k = 0, 1, \dots, N$ , we define

$$\mathfrak{T}_k := \{\mathbb{T} | \mathbb{T} \subseteq \mathbb{U}, |\mathbb{T}| = k\}, \quad \mathfrak{T}_k^* := \cup_{i=1, \dots, k} \mathfrak{T}_i.$$

The ANOVA decomposition of  $u(\mathbf{x}, \boldsymbol{\mu})$  is then given by

$$\begin{aligned} u(\mathbf{x}, \boldsymbol{\mu}) &= u_0(\mathbf{x}) + \sum_{\mathbb{T} \in \mathfrak{T}_N^*} u_{\mathbb{T}}(\mathbf{x}, \boldsymbol{\mu}_{\mathbb{T}}) \\ &= u_0(\mathbf{x}) + \sum_{\mathbb{T} \in \mathfrak{T}_1} u_{\mathbb{T}}(\mathbf{x}, \boldsymbol{\mu}_{\mathbb{T}}) + \dots + \sum_{\mathbb{T} \in \mathfrak{T}_N} u_{\mathbb{T}}(\mathbf{x}, \boldsymbol{\mu}_{\mathbb{T}}), \end{aligned} \quad (3.9)$$

where  $u_0(\mathbf{x})$  and  $u_{\mathbb{T}}(\mathbf{x}, \boldsymbol{\mu}_{\mathbb{T}})$  are defined such that

$$u_0(\mathbf{x}) = \int_{\Gamma} \rho(\boldsymbol{\mu}) u(\mathbf{x}, \boldsymbol{\mu}) d\boldsymbol{\mu}, \quad (3.10)$$

$$\int_{\Gamma_{t_k}} \rho_{t_k}(\mu_{t_k}) u_{\mathbb{T}}(\mathbf{x}, \boldsymbol{\mu}_{\mathbb{T}}) d\mu_{t_k} = 0, \quad k = 1, \dots, t_{|\mathbb{T}|}. \quad (3.11)$$

We call  $u_{\mathbb{T}}(\mathbf{x}, \boldsymbol{\mu}_{\mathbb{T}})$  in (3.9) the  $|\mathbb{T}|$ -th order term or  $|\mathbb{T}|$ -th order component function, and call  $u_0(\mathbf{x})$  the 0-th order term or 0-th order component function for special case.

An important property of the ANOVA decomposition is that all the terms in (3.9) are orthogonal, as follows from (3.11). Thus, the variance of  $u(\mathbf{x}, \boldsymbol{\mu})$  is the sum of the variances of all the decomposition terms:

$$\text{V}[u] = \sum_{j=1}^N \sum_{\mathbb{T} \in \mathfrak{T}_k} \text{V}[u_{\mathbb{T}}(\mathbf{x}, \boldsymbol{\mu}_{\mathbb{T}})], \quad (3.12)$$

where

$$\text{V}[u_{\mathbb{T}}(\mathbf{x}, \boldsymbol{\mu}_{\mathbb{T}})] = \int_{\Gamma} \rho(\boldsymbol{\mu}) u_{\mathbb{T}}^2(\mathbf{x}, \boldsymbol{\mu}_{\mathbb{T}}) d\boldsymbol{\mu} = \int_{\Gamma_{\mathbb{T}}} \rho_{\mathbb{T}}(\boldsymbol{\mu}_{\mathbb{T}}) u_{\mathbb{T}}^2(\mathbf{x}, \boldsymbol{\mu}_{\mathbb{T}}) d\boldsymbol{\mu}_{\mathbb{T}}, \quad (3.13)$$

here and hereafter

$$\rho_{\mathbb{T}}(\boldsymbol{\mu}_{\mathbb{T}}) = \rho_{t_1}(\mu_{t_1}) \cdots \rho_{t_{|\mathbb{T}|}}(\mu_{t_{|\mathbb{T}|}}), \quad \Gamma_{\mathbb{T}} = \Gamma_{t_1} \times \cdots \times \Gamma_{t_{|\mathbb{T}|}}, \quad |\mathbb{T}| > 0.$$

### 3.4 Adaptive ANOVA decomposition

Note that the  $k$ -th order term in (3.9), i.e.,  $\sum_{\mathbb{T} \in \mathfrak{T}_k} u_{\mathbb{T}}(\mathbf{x}, \boldsymbol{\mu}_{\mathbb{T}})$ , has  $\binom{N}{k}$  terms. For high dimensional problems, the total number of terms in (3.9) can be prohibitively large. This motivates the development of an adaptive ANOVA expansion for such problems. The adaptive ANOVA approach is expected to be a more efficient way to approximate the exact solution since only part of low order terms in (3.9) is activated based on certain criteria [27].

To determine which terms to include in the ANOVA decomposition, we define sensitivity indices for each term as follows:

$$\mathfrak{S}_{\mathbb{T}} = \frac{\|V[u_{\mathbb{T}}]\|_{L^2(D)}}{\sum_{\mathbb{T} \in \mathfrak{T}_N^*} \|V[u_{\mathbb{T}}]\|_{L^2(D)}},$$

where  $\|\cdot\|_{L^2(D)}$  denotes the  $L^2$  function norm. It follows from equations (3.12)–(3.13) that

$$0 \leq \mathfrak{S}_{\mathbb{T}} \leq 1, \quad \sum_{\mathbb{T} \in \mathfrak{T}_N^*} \mathfrak{S}_{\mathbb{T}} = 1.$$

The intuitive way to select the important terms in the ANOVA decomposition (3.9) is that find the terms such that  $\mathfrak{S}_{\mathbb{T}} \geq \text{TOL}$ , where  $\text{TOL}$  is a given tolerance. However, computing all possible terms is computationally expensive since  $u(\mathbf{x}, \boldsymbol{\mu})$  is the solution of a PDE with random inputs. Instead, we construct the higher order component functions based on the lower order terms in the following way.

Let  $\mathfrak{J}_k \subseteq \mathfrak{T}_k$  denote the sets of active indices for each order. Using these active indices, the solution  $u(\mathbf{x}, \boldsymbol{\mu})$  can be approximated by

$$u(\mathbf{x}, \boldsymbol{\mu}) \approx u_0(\mathbf{x}) + \sum_{\mathbb{T} \in \mathfrak{J}_1} u_{\mathbb{T}}(\mathbf{x}, \boldsymbol{\mu}_{\mathbb{T}}) + \sum_{\mathbb{T} \in \mathfrak{J}_2} u_{\mathbb{T}}(\mathbf{x}, \boldsymbol{\mu}_{\mathbb{T}}) + \dots$$

For the first order terms, all the terms are retained, i.e.,  $\mathfrak{J}_1 = \mathfrak{T}_1$ . Suppose that  $\mathfrak{J}_k$  is given for  $k \leq N - 1$ , and define the relative variance  $\gamma_{\mathbb{T}}$  as

$$\gamma_{\mathbb{T}} := \frac{\|V[u_{\mathbb{T}}]\|_{L^2(D)}}{\sum_{\mathbb{T} \in \mathfrak{J}_k^*} \|V[u_{\mathbb{T}}]\|_{L^2(D)}}, \quad \mathbb{T} \in \mathfrak{J}_k^*, \quad (3.14)$$

where  $\mathfrak{J}_k^* := \mathfrak{J}_1 \cup \dots \cup \mathfrak{J}_k$ . Then, the index set of the next order can be constructed via

$$\mathfrak{J}_{k+1} := \{\mathbb{T} | \mathbb{T} \in \mathfrak{T}_{k+1}, \text{ and } \forall \mathbb{S} \subseteq \mathbb{T} \text{ with } |\mathbb{S}| = k \text{ satisfies } \mathbb{S} \in \tilde{\mathfrak{J}}_k\},$$

where

$$\tilde{\mathfrak{J}}_k := \{\mathbb{T} \in \mathfrak{J}_k | \gamma_{\mathbb{T}} \geq \text{TOL}\}.$$

---

#### Algorithm 1 Adaptive ANOVA decomposition

---

**Input:**  $u(\mathbf{x}, \boldsymbol{\mu})$  and  $\text{TOL}$ , set  $k = 1$  and  $\mathfrak{J}_1 = \{\{1\}, \dots, \{N\}\}$ .  
**while** ( $k < N$ ) and  $\mathfrak{J}_k \neq \emptyset$  **do**  
    Compute  $\gamma_{\mathbb{T}}$  for  $\mathbb{T} \in \mathfrak{J}_k$ .  
    Set  $\tilde{\mathfrak{J}}_k := \{\mathbb{T} \in \mathfrak{T}_k | \gamma_{\mathbb{T}} \geq \text{TOL}\}$ .  
    Set  $\mathfrak{J}_{k+1} := \{\mathbb{T} | \mathbb{T} \in \mathfrak{T}_{k+1}, \text{ and } \forall \mathbb{S} \subseteq \mathbb{T} \text{ with } |\mathbb{S}| = k \text{ satisfies } \mathbb{S} \in \tilde{\mathfrak{J}}_k\}$ .  
     $k = k + 1$ .  
**end while**

---

Algorithm 1 presents the pseudo-code for the adaptive ANOVA decomposition. However, computing the relative variance  $\gamma_{\mathbb{T}}$  efficiently by classical methods can be challenging, especially when dealing with the high dimensional random inputs that arise in the context of PDEs with random inputs. To address this issue, we propose an adaptive ANOVA stochastic Galerkin method. In the following sections, we provide details of how to compute the relative variance  $\gamma_{\mathbb{T}}$  in the adaptive ANOVA stochastic Galerkin method.

## 4 Adaptive ANOVA stochastic Galerkin method

In the last section, we introduced the ANOVA decomposition as a method to capture the important features of the solution. By representing the component functions of the ANOVA decomposition as the generalized polynomials chaos expansion, an effective surrogate model for the problem (2.1) can be constructed, which is essential for accelerating the solution evaluation process for time intensive problems. There are two widely used approaches for this purpose: the generalized polynomial chaos (gPC) expansion [24], and the polynomial dimensional decomposition (PDD) [19]. In this work, we apply the gPC expansion to present the component functions in (3.9). However, it is noteworthy that the PDD can also be used similarly.

### 4.1 Generalized polynomial chaos expansion of component functions

Let us commence with the definition of gPC basis functions for a single random variable. Suppose that  $\mu_k$  is a random variable with probability density function  $\rho_k(\mu_k)$ , where  $k = 1, \dots, N$ . The gPC basis functions are the orthogonal polynomials satisfying

$$\int_{\Gamma_{t_k}} \rho_k(\mu_k) \phi_i^{(k)}(\mu_k) \phi_j^{(k)}(\mu_k) d\mu_k = \delta_{i,j}, \quad (4.1)$$

where  $i$  and  $j$  are non-negative integers, and  $\delta_{i,j}$  is the Kronecker delta.

For  $N$  dimensional random variables, let  $\mathbf{i} = (i_1, \dots, i_N) \in \mathbb{N}^N$  be a multi-index with the total degree  $|\mathbf{i}| = i_1 + \dots + i_N$ . Note that in this work, we assume that the components of  $\boldsymbol{\mu}$ , i.e.,  $\mu_1, \dots, \mu_N$  are mutually independent, and thus the  $N$ -variate gPC basis functions are the products of the univariate gPC polynomials, i.e.,

$$\Phi_{\mathbf{i}}(\boldsymbol{\mu}) = \phi_{i_1}^{(1)}(\mu_1) \cdots \phi_{i_N}^{(N)}(\mu_N).$$

It follows from (4.1) that

$$\int_{\Gamma} \rho(\boldsymbol{\mu}) \Phi_{\mathbf{i}}(\boldsymbol{\mu}) \Phi_{\mathbf{j}}(\boldsymbol{\mu}) d\boldsymbol{\mu} = \delta_{\mathbf{i},\mathbf{j}},$$

where  $\delta_{\mathbf{i},\mathbf{j}} = \delta_{i_1,j_1} \cdots \delta_{i_N,j_N}$ .

We now consider the generalized polynomial chaos expansion of the  $|\mathbb{T}|$ -th order component function  $u_{\mathbb{T}}(\mathbf{x}, \boldsymbol{\mu}_{\mathbb{T}})$ , which requires some notations. Let  $\mathbb{T}^c = \{t_1^c, \dots, t_{|\mathbb{T}^c|}^c\}$  be the complementary set of  $\mathbb{T}$ , i.e.,  $\mathbb{T}^c = \mathbb{U}/\mathbb{T}$ , where the universal set is given by  $\mathbb{U} = \{1, \dots, N\}$ . For any set  $\mathbb{T} \subseteq \mathbb{U}$  with  $|\mathbb{T}| > 0$ , the gPC basis function corresponding to the multi-index  $\mathbf{i}_{\mathbb{T}}$  is given by

$$\Phi_{\mathbf{i}_{\mathbb{T}}}(\boldsymbol{\mu}_{\mathbb{T}}) = \phi_{i_{t_1}}^{(t_1)}(\mu_{t_1}) \cdots \phi_{i_{t_{|\mathbb{T}|}}}^{(t_{|\mathbb{T}|})}(\mu_{t_{|\mathbb{T}|}}),$$

where  $\mathbf{i}_{\mathbb{T}}$  denote the multi-index that contains the components of the multi-index  $\mathbf{i}$  indexed by  $\mathbb{T}$ , i.e.,  $\mathbf{i}_{\mathbb{T}} = (i_{t_1}, \dots, i_{t_{|\mathbb{T}|}})$ . In additional, let  $\mathfrak{M}_{\mathbb{T}}$  be the set of multi-indices defined by

$$\mathfrak{M}_{\mathbb{T}} := \{\mathbf{i} | \mathbf{i} \in \mathbb{N}^N, i_{t_1} \neq 0, \dots, i_{t_{|\mathbb{T}|}} \neq 0, i_{t_1^c} = 0, \dots, i_{t_{|\mathbb{T}^c|}^c} = 0\}, \quad 0 < |\mathbb{T}| < N.$$

For the special case  $|\mathbb{T}| = 0$ , we set  $\mathfrak{M}_{\mathbb{T}} = \{\mathbf{i} | \mathbf{i} \in \mathbb{N}^N, i(1) = 0, \dots, i(N) = 0\}$ , and for the special case  $|\mathbb{T}| = N$ , we set  $\mathfrak{M}_{\mathbb{T}} := \{\mathbf{i} | \mathbf{i} \in \mathbb{N}^N, i(1) \neq 0, \dots, i(N) \neq 0\}$ . We can then state the following theorem:



**Theorem 4.1** *Given  $\mathbf{x} \in D$  and  $\mathbb{T} \subseteq \mathbb{U}$  with  $|\mathbb{T}| > 0$ , assuming that the  $|\mathbb{T}|$ -th order component function  $u_{\mathbb{T}}(\mathbf{x}, \boldsymbol{\mu}_{\mathbb{T}})$  belongs to  $L^2_{\rho}(I)$ , then the generalized polynomial chaos expansion of  $u_{\mathbb{T}}(\mathbf{x}, \boldsymbol{\mu}_{\mathbb{T}})$  can be expressed by*

$$u_{\mathbb{T}}(\mathbf{x}, \boldsymbol{\mu}_{\mathbb{T}}) = \sum_{\mathbf{i} \in \mathfrak{M}_{\mathbb{T}}} u_{\mathbf{i}}(\mathbf{x}) \Phi_{\mathbf{i}}(\boldsymbol{\mu}), \quad (4.2)$$

where  $u_{\mathbf{i}}(\mathbf{x})$  is the coefficient of  $\Phi_{\mathbf{i}}(\boldsymbol{\mu})$  defined by

$$u_{\mathbf{i}}(\mathbf{x}) = \int_{\Gamma} \rho(\boldsymbol{\mu}) u_{\mathbb{T}}(\mathbf{x}, \boldsymbol{\mu}_{\mathbb{T}}) \Phi_{\mathbf{i}}(\boldsymbol{\mu}) d\boldsymbol{\mu}.$$

*Proof* Since  $u_{\mathbb{T}}(\mathbf{x}, \boldsymbol{\mu}_{\mathbb{T}}) \in L^2_{\rho}(I)$  and  $\{\Phi_{|\mathbf{i}|}\}_{|\mathbf{i}|=0}^{\infty}$  forms a complete orthonormal basis of  $L^2_{\rho}(I)$ , we can express the generalized polynomial chaos expansion of  $u_{\mathbb{T}}(\mathbf{x}, \boldsymbol{\mu}_{\mathbb{T}})$  as

$$u_{\mathbb{T}}(\mathbf{x}, \boldsymbol{\mu}_{\mathbb{T}}) = \sum_{|\mathbf{i}|=0}^{\infty} u_{\mathbf{i}}(\mathbf{x}) \Phi_{\mathbf{i}}(\boldsymbol{\mu}), \quad (4.3)$$

where  $u_{\mathbf{i}}(\mathbf{x})$  are the coefficients of the expansion given by

$$u_{\mathbf{i}}(\mathbf{x}) = \int_{\Gamma} \rho(\boldsymbol{\mu}) u_{\mathbb{T}}(\mathbf{x}, \boldsymbol{\mu}_{\mathbb{T}}) \Phi_{\mathbf{i}}(\boldsymbol{\mu}) d\boldsymbol{\mu}.$$

To prove the theorem, it suffices to show that if  $\mathbf{i} \notin \mathfrak{M}_{\mathbb{T}}$ , which means that there exists  $t_k \in \mathbb{T}$  such that  $\mathbf{i}(t_k) = 0$  or there exists  $t_k^c \in \mathbb{T}^c$  such that  $\mathbf{i}(t_k^c) \neq 0$ , then  $u_{\mathbf{i}}(\mathbf{x}) = 0$ .

If there exists  $t_k \in \mathbb{T}$  such that  $\mathbf{i}(t_k) = 0$ , let  $\mathbb{S} = \mathbb{U} / \{t_k\}$  be the complementary set of  $\{t_k\}$ , and note that  $\phi_0^{(t_k)}(\mu_{t_k}) = 1$ . Then, we have

$$\begin{aligned} \int_{\Gamma} \rho(\boldsymbol{\mu}) u_{\mathbb{T}}(\mathbf{x}, \boldsymbol{\mu}_{\mathbb{T}}) \Phi_{\mathbf{i}}(\boldsymbol{\mu}) d\boldsymbol{\mu} &= \int_{\Gamma_{\mathbb{S}}} \int_{\Gamma_{t_k}} \rho_{\mathbb{S}}(\boldsymbol{\mu}_{\mathbb{S}}) \rho_{t_k}(\mu_{t_k}) \Phi_{\mathbf{i}_{\mathbb{S}}}(\boldsymbol{\mu}_{\mathbb{S}}) u_{\mathbb{T}}(\mathbf{x}, \boldsymbol{\mu}_{\mathbb{T}}) d\mu_{t_k} d\boldsymbol{\mu}_{\mathbb{S}} \\ &= \int_{\Gamma_{\mathbb{S}}} \left( \rho_{\mathbb{S}}(\boldsymbol{\mu}_{\mathbb{S}}) \Phi_{\mathbf{i}_{\mathbb{S}}}(\boldsymbol{\mu}_{\mathbb{S}}) \int_{\Gamma_{t_k}} \rho_{t_k}(\mu_{t_k}) u_{\mathbb{T}}(\mathbf{x}, \boldsymbol{\mu}_{\mathbb{T}}) d\mu_{t_k} \right) d\boldsymbol{\mu}_{\mathbb{S}}. \end{aligned}$$

Using (3.11), we obtain

$$\int_{\Gamma_{t_k}} \rho_{t_k}(\mu_{t_k}) u_{\mathbb{T}}(\mathbf{x}, \boldsymbol{\mu}_{\mathbb{T}}) d\mu_{t_k} = 0,$$

which implies that

$$u_{\mathbf{i}}(\mathbf{x}) = \int_{\Gamma} \rho(\boldsymbol{\mu}) u_{\mathbb{T}}(\mathbf{x}, \boldsymbol{\mu}_{\mathbb{T}}) \Phi_{\mathbf{i}}(\boldsymbol{\mu}) d\boldsymbol{\mu} = 0.$$

On the other hand, if there exists  $t_k^c \in \mathbb{T}^c$  such that  $\mathbf{i}(t_k^c) \neq 0$ , then we have

$$\begin{aligned} \int_{\Gamma} \rho(\boldsymbol{\mu}) u_{\mathbb{T}}(\mathbf{x}, \boldsymbol{\mu}_{\mathbb{T}}) \Phi_{\mathbf{i}}(\boldsymbol{\mu}) d\boldsymbol{\mu} &= \int_{\Gamma_{\mathbb{T}}} \int_{\Gamma_{\mathbb{T}^c}} \rho_{\mathbb{T}}(\boldsymbol{\mu}_{\mathbb{T}}) \rho_{\mathbb{T}^c}(\boldsymbol{\mu}_{\mathbb{T}^c}) u_{\mathbb{T}}(\mathbf{x}, \boldsymbol{\mu}_{\mathbb{T}}) \Phi_{\mathbf{i}_{\mathbb{T}}}(\boldsymbol{\mu}_{\mathbb{T}}) \Phi_{\mathbf{i}_{\mathbb{T}^c}}(\boldsymbol{\mu}_{\mathbb{T}^c}) d\boldsymbol{\mu}_{\mathbb{T}} d\boldsymbol{\mu}_{\mathbb{T}^c} \\ &= \int_{\Gamma_{\mathbb{T}}} \rho_{\mathbb{T}}(\boldsymbol{\mu}_{\mathbb{T}}) u_{\mathbb{T}}(\mathbf{x}, \boldsymbol{\mu}_{\mathbb{T}}) \Phi_{\mathbf{i}_{\mathbb{T}}}(\boldsymbol{\mu}_{\mathbb{T}}) d\boldsymbol{\mu}_{\mathbb{T}} \int_{\Gamma_{\mathbb{T}^c}} \rho_{\mathbb{T}^c}(\boldsymbol{\mu}_{\mathbb{T}^c}) \Phi_{\mathbf{i}_{\mathbb{T}^c}}(\boldsymbol{\mu}_{\mathbb{T}^c}) d\boldsymbol{\mu}_{\mathbb{T}^c}. \end{aligned}$$

Note that since the gPC basis function corresponding to  $(0, \dots, 0)$  is 1, and  $\mathbf{i}_{\mathbb{T}^c} \neq (0, \dots, 0)$ , we have

$$\int_{\Gamma_{\mathbb{T}^c}} \rho_{\mathbb{T}^c}(\boldsymbol{\mu}_{\mathbb{T}^c}) \Phi_{\mathbf{i}_{\mathbb{T}^c}}(\boldsymbol{\mu}_{\mathbb{T}^c}) d\boldsymbol{\mu}_{\mathbb{T}^c} = 0,$$

and thus

$$u_{\mathbf{i}}(\mathbf{x}) = \int_{\Gamma} \rho(\boldsymbol{\mu}) u_{\mathbb{T}}(\mathbf{x}, \boldsymbol{\mu}_{\mathbb{T}}) \Phi_{\mathbf{i}}(\boldsymbol{\mu}) d\boldsymbol{\mu} = 0.$$

**Theorem 4.2** *Suppose that  $u(\mathbf{x}, \boldsymbol{\mu})$  can be expressed as*

$$u(\mathbf{x}, \boldsymbol{\mu}) = u_0(\mathbf{x}) + \sum_{\mathbb{T} \in \mathfrak{T}_1} u_{\mathbb{T}}(\mathbf{x}, \boldsymbol{\mu}_{\mathbb{T}}) + \dots + \sum_{\mathbb{T} \in \mathfrak{T}_N} u_{\mathbb{T}}(\mathbf{x}, \boldsymbol{\mu}_{\mathbb{T}}), \quad (4.4)$$

where

$$u_{\mathbb{T}}(\mathbf{x}, \boldsymbol{\mu}_{\mathbb{T}}) = \sum_{\mathbf{i} \in \mathfrak{M}_{\mathbb{T}}} u_{\mathbf{i}}(\mathbf{x}) \Phi_{\mathbf{i}}(\boldsymbol{\mu}), \quad \mathbb{T} \in \mathfrak{T}_N^*. \quad (4.5)$$

Then the right hand side of (4.4) is the ANOVA decomposition of  $u(\mathbf{x}, \boldsymbol{\mu})$ .

*Proof* To complete the proof, we only need to show that the right hand side of (4.4) satisfies (3.10) and (3.11). Using (4.5), we have

$$\begin{aligned} \int_{\Gamma} \rho(\boldsymbol{\mu}) u(\mathbf{x}, \boldsymbol{\mu}) d\boldsymbol{\mu} &= \int_{\Gamma} \rho(\boldsymbol{\mu}) u_0(\mathbf{x}) d\boldsymbol{\mu} + \sum_{\mathbb{T} \in \mathfrak{T}_N^*} \int_{\Gamma} \rho(\boldsymbol{\mu}) u_{\mathbb{T}}(\mathbf{x}, \boldsymbol{\mu}_{\mathbb{T}}) d\boldsymbol{\mu} \\ &= u_0(\mathbf{x}) + \sum_{\mathbb{T} \in \mathfrak{T}_N^*} \sum_{\mathbf{i} \in \mathfrak{M}_{\mathbb{T}}} u_{\mathbf{i}}(\mathbf{x}) \int_{\Gamma} \rho(\boldsymbol{\mu}) \Phi_{\mathbf{i}}(\boldsymbol{\mu}) d\boldsymbol{\mu}. \end{aligned}$$

Since  $\mathbb{T} \neq \emptyset$  when  $\mathbb{T} \in \mathfrak{T}_N^*$ , we have

$$\mathbf{i} \neq (0, \dots, 0), \quad \mathbf{i} \in \mathfrak{M}_{\mathbb{T}}.$$

Thus,

$$\int_{\Gamma} \rho(\boldsymbol{\mu}) \Phi_{\mathbf{i}}(\boldsymbol{\mu}) d\boldsymbol{\mu} = 0,$$

which implies that

$$\int_{\Gamma} \rho(\boldsymbol{\mu}) u(\mathbf{x}, \boldsymbol{\mu}) d\boldsymbol{\mu} = u_0(\mathbf{x}).$$

To show that the right hand side of (4.4) satisfies (3.11), suppose that  $t_k \in \mathbb{T}$ ,  $k = 1, \dots, t_{|\mathbb{T}|}$ , and let  $\mathbb{S} = \mathbb{U} / \{t_k\}$  be the complementary set of  $\{t_k\}$ . Then, by (4.5), we have

$$\begin{aligned} \int_{\Gamma_{t_k}} \rho_{t_k}(\mu_{t_k}) u_{\mathbb{T}}(\mathbf{x}, \boldsymbol{\mu}_{\mathbb{T}}) d\mu_{t_k} &= \sum_{\mathbf{i} \in \mathfrak{M}_{\mathbb{T}}} u_{\mathbf{i}}(\mathbf{x}) \int_{\Gamma_{t_k}} \rho_{t_k}(\mu_{t_k}) \Phi_{\mathbf{i}}(\boldsymbol{\mu}) d\mu_{t_k} \\ &= \sum_{\mathbf{i} \in \mathfrak{M}_{\mathbb{T}}} u_{\mathbf{i}}(\mathbf{x}) \Phi_{\mathbf{i}_{\mathbb{S}}}(\boldsymbol{\mu}_{\mathbb{S}}) \int_{\Gamma_{t_k}} \rho_{t_k}(\mu_{t_k}) \phi_{\mathbf{i}_{\mathbb{T}}^{(t_k)}}(\mu_{t_k}) d\mu_{t_k} \end{aligned}$$

Recall that  $\phi_0^{(t_k)}(\mu_{t_k}) = 1$  and  $\mathbf{i}(t_k) \neq 0$ , we have

$$\int_{\Gamma_{t_k}} \rho_{t_k}(\mu_{t_k}) \phi_{\mathbf{i}(t_k)}^{(t_k)}(\mu_{t_k}) d\mu_{t_k} = 0,$$

which implies that

$$\int_{\Gamma_{t_k}} \rho_{t_k}(\mu_{t_k}) u_{\mathbb{T}}(\mathbf{x}, \boldsymbol{\mu}_{\mathbb{T}}) d\mu_{t_k} = 0, \quad k = 1, \dots, t_{|\mathbb{T}|}.$$

In practical computations, the expansion given in (4.2) must be truncated to a finite number of terms. Following the approach in [22], we retain the terms with the total degree up to  $p$ . This yields the approximation

$$u_{\mathbb{T}}(\mathbf{x}, \boldsymbol{\mu}_{\mathbb{T}}) \approx \sum_{\mathbf{i} \in \mathfrak{M}_{\mathbb{T}}^p} u_{\mathbf{i}}(\mathbf{x}) \Phi_{\mathbf{i}}(\boldsymbol{\mu}), \quad (4.6)$$

where  $\mathfrak{M}_{\mathbb{T}}^p$  is the set of multi-indices defined by

$$\mathfrak{M}_{\mathbb{T}}^p := \{\mathbf{i} | \mathbf{i} \in \mathfrak{M}_{\mathbb{T}} \text{ and } |\mathbf{i}| \leq p\}.$$

By inserting (4.6) into (3.9), we obtain the following expansion of  $u(\mathbf{x}, \boldsymbol{\mu})$  in terms of gPC basis functions:

$$u(\mathbf{x}, \boldsymbol{\mu}) \approx u_p(\mathbf{x}, \boldsymbol{\mu}) = u_0(\mathbf{x}) + \sum_{\mathbb{T} \in \mathfrak{T}_1} \sum_{\mathbf{i} \in \mathfrak{M}_{\mathbb{T}}^p} u_{\mathbf{i}}(\mathbf{x}) \Phi_{\mathbf{i}}(\boldsymbol{\mu}) + \dots + \sum_{\mathbb{T} \in \mathfrak{T}_N} \sum_{\mathbf{i} \in \mathfrak{M}_{\mathbb{T}}^p} u_{\mathbf{i}}(\mathbf{x}) \Phi_{\mathbf{i}}(\boldsymbol{\mu}), \quad (4.7)$$

where  $u_p(\mathbf{x}, \boldsymbol{\mu})$  is the polynomial approximation of  $u(\mathbf{x}, \boldsymbol{\mu})$  with the total degree up to  $p$ . We can easily compute the variance of each term in (4.7) using the following expression:

$$\text{V}[u_{\mathbb{T}}] \approx \sum_{\mathbb{T} \in \mathfrak{T}_N^*} \sum_{\mathbf{i} \in \mathfrak{M}_{\mathbb{T}}^p} u_{\mathbf{i}}^2(\mathbf{x}). \quad (4.8)$$

Figure 4.1 illustrates the multi-indices of the gPC basis functions corresponding to the component functions of each order in (4.7). It is worth noting that the number of terms in (4.7) is given by

$$\binom{N}{0} \binom{p}{0} + \dots + \binom{N}{N} \binom{p}{N} = \binom{N+p}{N}, \quad (4.9)$$

which identical to the number of terms in the generalized polynomial chaos expansion with the total degree up to  $p$ . The equation (4.9) is commonly referred to as the Vandermonde's identity or the Vandermonde's convolution. Interested readers can find more information on this topic in the relevant literature, such as [2].

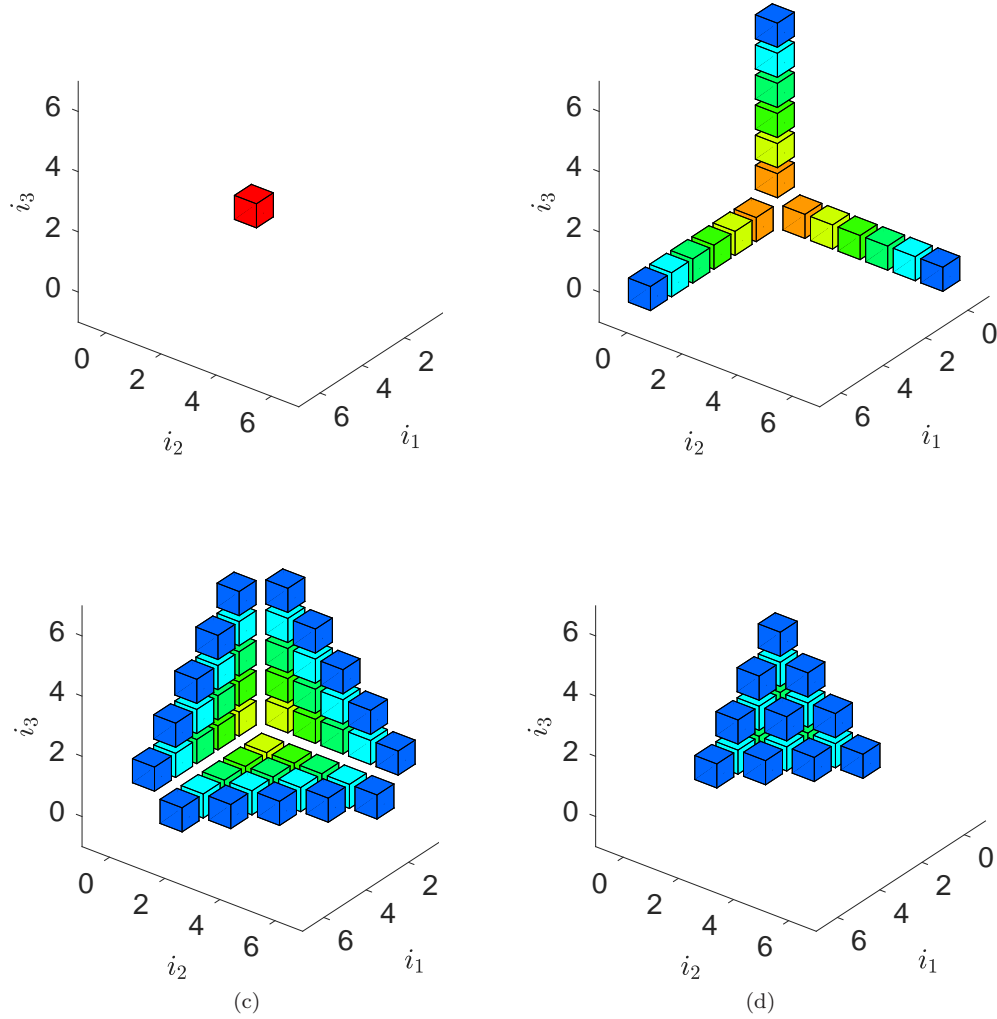


Fig. 4.1: Multi-indices of the gPC basis functions corresponding to the component functions of each order in 3 dimensions with the total degree up to 6, arranged according to the order of the component functions (from left to right): 0-th, first, second, and third order.

#### 4.2 Adaptive ANOVA stochastic Galerkin method

Based on the adaptive ANOVA decomposition and the gPC expansion of component functions, we can develop an adaptive ANOVA stochastic Galerkin method for the problem (2.1). The idea is quite simple, namely, we select the basis functions of stochastic space based on the adaptive ANOVA decomposition, in which the relative variance is computed by (3.14) and (4.8).

**Algorithm 2** Adaptive ANOVA stochastic Galerkin method

**Input:** The gPC order  $p$  and the tolerance **TOL** in ANOVA decomposition.

Set  $k = 1$ ,  $\mathfrak{J}_0 = \emptyset$ ,  $\mathfrak{J}_1 = \{\{1\}, \dots, \{N\}\}$  and compute  $\mathbf{A}_i$  and  $\mathbf{f}$  defined in (3.8).

**while** ( $k < N$ ) and  $\mathfrak{J}_k \neq \emptyset$  **do**

    Generate the multi-indices  $\mathfrak{M}_k^{p\dagger}$  and compute  $\mathbf{G}_i$  and  $\mathbf{h}$  defined in (3.7).

    Solve the linear system (3.6) and compute  $\gamma_{\mathbb{T}}$  for  $\mathbb{T} \in \mathfrak{J}_k$  by (3.14) and (4.8).

    Set  $\tilde{\mathfrak{J}}_k := \{\mathbb{T} \in \mathfrak{J}_k \mid \gamma_{\mathbb{T}} \geq \text{TOL}\}$ .

    Set  $\mathfrak{J}_{k+1} := \{\mathbb{T} \mid \mathbb{T} \in \mathfrak{J}_{k+1}, \text{ and } \forall \mathbb{S} \subseteq \mathbb{T} \text{ with } |\mathbb{S}| = k \text{ satisfies } \mathbb{S} \in \tilde{\mathfrak{J}}_k\}$ .

$k = k + 1$ .

**end while**

**Return:** the approximation  $u^{\text{ap}}(\mathbf{x}, \boldsymbol{\mu})$ , the mean function  $u_0(\mathbf{x})$  and the variance function  $\sum_{i \in \mathfrak{M}_T^{p*}} u_i^2(\mathbf{x})$

To give the algorithm of this procedure, some notations are needed. We first collect the basis functions associated with the  $k$ -th order component function  $u_{\mathbb{T}}(\mathbf{x}, \boldsymbol{\mu}_{\mathbb{T}})$  and denote the set of their multi-indices with the total degree up to  $p$  as  $\mathfrak{M}_k^p := \cup_{\mathbb{T} \in \mathfrak{J}_k} \mathfrak{M}_{\mathbb{T}}^p$ . Moreover, let us denote the set of all multi-indices as  $\mathfrak{M}_k^{p\dagger} := \mathfrak{M}_{\emptyset} \cup \mathfrak{M}_k^{p*}$ , where  $\mathfrak{M}_k^{p*} := \cup_{\mathbb{T} \in \mathfrak{J}_k^*} \mathfrak{M}_{\mathbb{T}}^p$ . With those notations, Algorithm 2 gives the pseudo code for the adaptive ANOVA stochastic Galerkin method.

In the adaptive ANOVA stochastic Galerkin method, we select the set of multi-indices adaptively based on the ANOVA decomposition. Specifically, only part of the multi-indices with the total degree up to  $p$  will be retained, resulting in a much lower computational cost compared to the standard stochastic Galerkin method. It is worth noting that if the tolerance **TOL** is chosen small enough, all multi-indices will be selected, and the adaptive ANOVA stochastic Galerkin method will become equivalent to the standard stochastic Galerkin method.

## 5 Numerical results

In this section, we will explore two problems: a diffusion problem and a Helmholtz problem. All the results presented here are obtained using MATLAB R2015b on a desktop with a 2.90GHz Intel Core i7-10700 CPU. The CPU time reported in this paper correspond to the total time required to solve the linear systems in the respective procedures.

To assess the accuracy of the adaptive ANOVA stochastic Galerkin(AASG) method or the Monte Carlo method (MCM), we define the errors of the mean and the variance functions as follows:

$$\begin{aligned} E_{\text{ERR}} &= \frac{\|E[u_{\text{REF}}(\mathbf{x}, \boldsymbol{\mu})] - E[u^{\text{ap}}(\mathbf{x}, \boldsymbol{\mu})]\|_{L^2}}{\|E[u_{\text{REF}}(\mathbf{x}, \boldsymbol{\mu})]\|_{L^2}}, \\ V_{\text{ERR}} &= \frac{\|V[u_{\text{REF}}(\mathbf{x}, \boldsymbol{\mu})] - V[u^{\text{ap}}(\mathbf{x}, \boldsymbol{\mu})]\|_{L^2}}{\|V[u_{\text{REF}}(\mathbf{x}, \boldsymbol{\mu})]\|_{L^2}}. \end{aligned}$$

Here,  $u_{\text{REF}}(\mathbf{x}, \boldsymbol{\mu})$  is the reference solution, and  $u^{\text{ap}}(\mathbf{x}, \boldsymbol{\mu})$  is the approximate solution.

### 5.1 Test problem 1

In this problem, we investigate the diffusion equation with random inputs, given by

$$\begin{aligned} -\nabla \cdot (a(\mathbf{x}, \boldsymbol{\mu}) \nabla u(\mathbf{x}, \boldsymbol{\mu})) &= 1 \quad \text{in } D \times \Gamma, \\ u(\mathbf{x}, \boldsymbol{\mu}) &= 0 \quad \text{on } \partial D \times \Gamma, \end{aligned}$$

where  $\partial u / \partial n$  denotes the outward normal derivative of  $u$  on the boundaries,  $D = [0, 1] \times [0, 1]$  is the spatial domain, and  $\partial D$  represents the boundary of  $D$ . The diffusion coefficient  $a(\mathbf{x}, \boldsymbol{\mu})$  is modeled as a truncated Karhunen–Loève (KL) expansion [11, 6] of a random field with a mean function  $a_0(\mathbf{x})$ , a standard deviation  $\sigma$ , and the covariance function  $\text{Cov}(\mathbf{x}, \mathbf{y})$  given by

$$\text{Cov}(\mathbf{x}, \mathbf{y}) = \sigma^2 \exp\left(-\frac{|x_1 - y_1|}{c} - \frac{|x_2 - y_2|}{c}\right),$$

where  $\mathbf{x} = [x_1, x_2]^T$ ,  $\mathbf{y} = [y_1, y_2]^T$  and  $c$  is the correlation length. The KL expansion takes the form

$$a(\mathbf{x}, \boldsymbol{\mu}) = a_0(\mathbf{x}) + \sum_{i=1}^N a_i(\mathbf{x}) \mu_i = a_0(\mathbf{x}) + \sum_{i=1}^N \sqrt{\lambda_i} c_i(\mathbf{x}) \mu_i, \quad (5.1)$$

where  $\{\lambda_i, c_i(\mathbf{x})\}_{i=1}^N$  are the eigenpairs of  $\text{Cov}(\mathbf{x}, \mathbf{y})$ ,  $\{\mu_i\}_{i=1}^N$  are uncorrelated random variables, and  $N$  is the number of KL modes retained.

For this test problem, we assume that the random variables  $\{\mu_i\}_{i=1}^N$  are independent and uniformly distributed within the range  $[-1, 1]$ . The parameters of  $a(\mathbf{x}, \boldsymbol{\mu})$  are set as shown in Table 5.1. The meshgrid in the physical domain is set to  $33 \times 33$  (i.e.,  $n_x = 33$ ), and the total degree of the gPC basis functions in the adaptive ANOVA stochastic Galerkin (AASG) method is set to  $p = 5$ . The linear systems arising from both the standard and the adaptive ANOVA stochastic Galerkin methods are solved using the preconditioned conjugate gradients (CG) method, with a tolerance of  $10^{-8}$  and the mean based preconditioner [15].

Table 5.1: Parameters of the diffusion coefficient  $a(\mathbf{x}, \boldsymbol{\mu})$  in (5.1) and  $K$  in (2.2).

Case	$a_0(\mathbf{x})$	$c$	$\sigma$	$N$	$K$
I	1	1/4	1/4	10	11
II	1	1/4	1/4	50	51

#### 5.1.1 Case I: a 10 dimensional diffusion problem

We consider the AASG method with decreasing tolerances  $\text{TOL} = \{10^{-1}, 10^{-3}, 10^{-5}, 10^{-7}, 10^{-9}\}$  to demonstrate its effectiveness and efficiency. To access the accuracy of the AASG method and MCM, we obtain the reference solution  $u_{\text{REF}}(\mathbf{x}, \boldsymbol{\mu})$  using the standard stochastic Galerkin method with the total degree of up to  $p = 7$ .

Table 5.2 presents the number of active indices for each order of the ANOVA decomposition and the total number of selected gPC basis functions in the stochastic space. We also report the

Table 5.2: Performance of the AASG method for different TOL .

TOL	$ \mathfrak{J}_1 $	$ \tilde{\mathfrak{J}}_1 $	$ \mathfrak{J}_2 $	$ \tilde{\mathfrak{J}}_2 $	$ \mathfrak{J}_3 $	$ \tilde{\mathfrak{J}}_3 $	$ \mathfrak{J}_4 $	$ \tilde{\mathfrak{J}}_4 $	$ \mathfrak{J}_5 $	$ \tilde{\mathfrak{J}}_5 $	$k$	$ \mathbf{m}_k^{5^\dagger} $	CPU time
$10^{-1}$	10	1	0	0	0	0	0	0	0	0	1	51	0.07
$10^{-3}$	10	10	45	2	0	0	0	0	0	0	2	501	0.88
$10^{-5}$	10	10	45	37	70	0	0	0	0	0	3	1201	3.36
$10^{-7}$	10	10	45	45	120	75	60	0	0	0	4	2001	9.34
$10^{-9}$	10	10	45	45	120	120	210	127	70	0	5	2821	18.90

computational time required for solving the resulting linear systems using the preconditioned CG method with a tolerance of  $10^{-8}$  and the mean based preconditioner. It can be observed that the number of selected gPC basis functions increases as the tolerance TOL decreases, and therefore, the accuracy can be improved by reducing TOL. For a 10 dimensional problem, the number of gPC basis functions with the total degree up to 5 is  $C_{15}^5 = 3003$ . From the table, it can be seen that when  $\text{TOL} = 10^{-9}$ , almost all the gPC basis functions are selected in the AASG method. Further decreasing the tolerance in the AASG method results in the selection of all gPC basis functions with the total degree up to 5, making the AASG method equivalent to the standard stochastic Galerkin method.

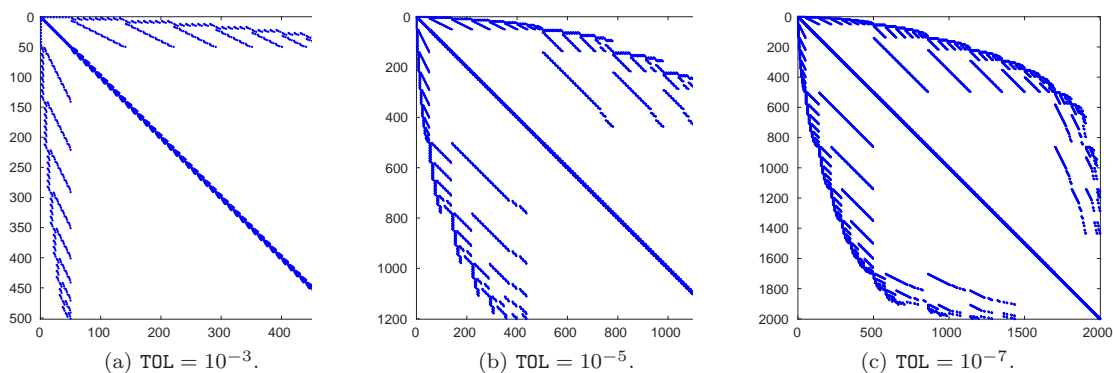
Fig. 5.1: Matrix block-structure (each block has dimension  $n_x \times n_x$ ) for  $\text{TOL} = 10^{-3}, 10^{-5}, 10^{-7}$ .

Figure 5.1 displays the block structure of the coefficient matrix of the resulting linear system. Each point in the figure represents a block of dimension  $n_x \times n_x$ . Furthermore, each nonzero block of the coefficient matrix has the same sparsity pattern as the corresponding deterministic problem. Therefore, the coefficient matrix is extremely large and sparse, and the resulting linear system should be solved using iterative methods.

Figure 5.2 displays the CPU time of the MCM and the AASG method as a function of the mean and the variance errors. The CPU time considered in this problem correspond to the total time of solving the linear systems in the respective procedures. The results indicate that the AASG method

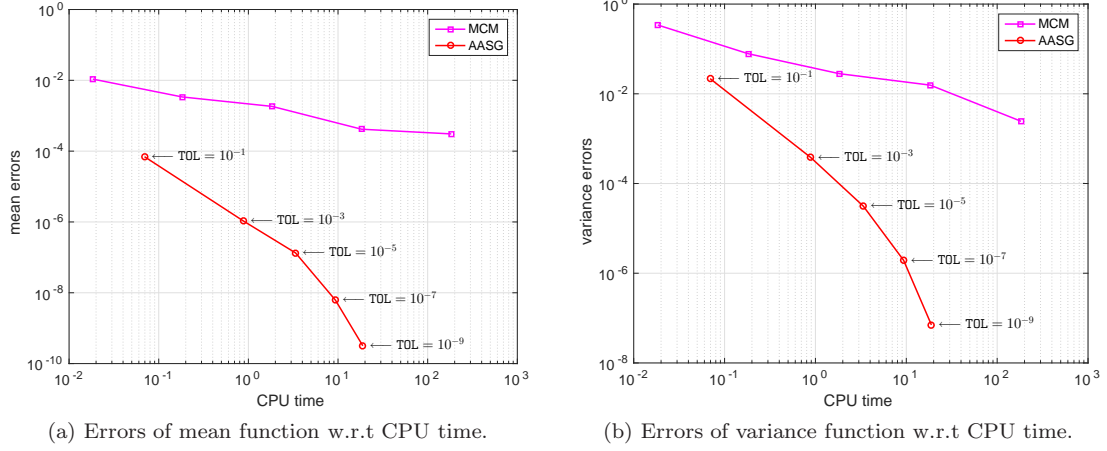


Fig. 5.2: Comparison of CPU time for the MCM and the AASG method.

is more efficient than MCM. It can be seen that the AASG method with a tolerance of  $\text{TOL} = 10^{-3}$  is more accurate than MCM with  $10^5$  samples.

### 5.1.2 Case II: a 50 dimensional diffusion problem

We consider the AASG method with decreasing tolerances  $\text{TOL} = \{10^{-1}, 10^{-2}, 10^{-3}, 10^{-4}, 10^{-5}\}$  to demonstrate its effectiveness and efficiency. To assess the accuracy of the AASG method and the MCM, we obtain the reference solution  $u_{\text{REF}}(\mathbf{x}, \boldsymbol{\mu})$  using the AASG method with a tolerance of  $\text{TOL} = 10^{-6}$ .

Table 5.3: Performance of the AASG method for different TOL .

TOL	$ \tilde{\mathcal{J}}_1 $	$ \tilde{\mathcal{J}}_1 $	$ \tilde{\mathcal{J}}_2 $	$ \tilde{\mathcal{J}}_2 $	$ \tilde{\mathcal{J}}_3 $	$ \tilde{\mathcal{J}}_3 $	$ \tilde{\mathcal{J}}_4 $	$ \tilde{\mathcal{J}}_4 $	$k$	$ \mathbf{m}_k^{5^\dagger} $	CPU time
$10^{-1}$	50	1	0	0	0	0	0	0	1	251	0.40
$10^{-2}$	50	11	55	0	0	0	0	0	2	801	2.01
$10^{-3}$	50	30	435	0	0	0	0	0	2	4601	14.77
$10^{-4}$	50	50	1225	15	8	0	0	0	3	12581	84.67
$10^{-5}$	50	50	1225	83	120	0	0	0	3	13701	88.95
$10^{-6}$	50	50	1225	377	1537	15	1	0	4	27876	279.19

Table 5.3 presents the number of active indices for each order of ANOVA decomposition and the total number of selected gPC basis functions in the stochastic space. We also report the computational time required for solving the resulting linear systems using the preconditioned CG method with a tolerance of  $10^{-8}$  and the mean based preconditioner. It can be observed that the number of



selected gPC basis functions increases as the tolerance TOL decreases, and therefore, the accuracy can be improved by reducing TOL. It is worth noting that the number of gPC basis functions with the total degree up to  $p = 5$  is  $C_{55}^5 = 3478761$ , which renders the standard stochastic Galerkin method practically infeasible for solving this problem in reasonable time.

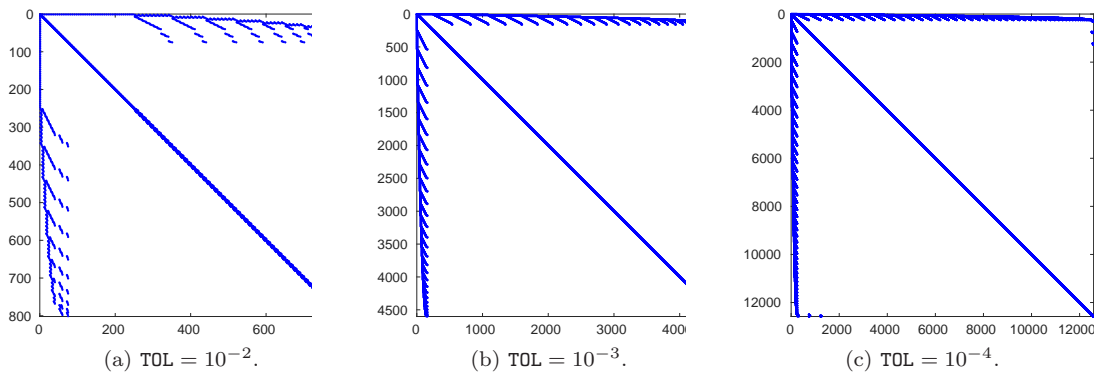


Fig. 5.3: Matrix block-structure (each block has dimension  $n_x \times n_x$ ) for TOL =  $10^{-2}, 10^{-3}, 10^{-4}$ .

Figure 5.3 displays the block structure of the coefficient matrix of the resulting linear system. Each point in the figure represents a block of dimension  $n_x \times n_x$ . Furthermore, each nonzero block of the coefficient matrix has the same sparsity pattern as the corresponding deterministic problem. It is evident from the figure that the coefficient matrix in this case exhibits a sparser pattern than that of Case I.

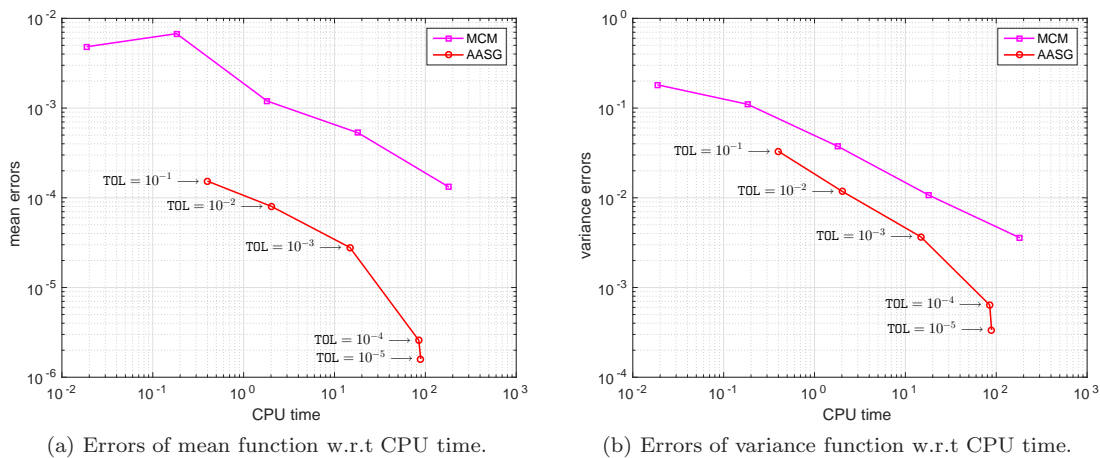


Fig. 5.4: Comparison of CPU time for the MCM and the AASG method.

The plot shown in Figure 5.4 compares the CPU time required by the MCM and the AASG method with respect to the mean and the variance errors. The results clearly indicate that the AASG method outperforms MCM in terms of efficiency. Specifically, we observe that the AASG method achieves a level of accuracy comparable to that of MCM with  $10^5$  samples, when a tolerance of  $\text{TOL} = 10^{-3}$  is used.

## 5.2 Test problem 2

In this test problem, we consider the stochastic Helmholtz problem given by

$$\nabla^2 u + a^2(\mathbf{x}, \boldsymbol{\mu})u = f(\mathbf{x}) \quad \text{in } D \times \Gamma,$$

with Sommerfeld radiation boundary condition. Here,  $D = [0, 1]^2$  is the domain of interest and the Helmholtz coefficient  $a(\mathbf{x}, \boldsymbol{\mu})$  is a truncated KL expansion of the random field given by

$$a(\mathbf{x}, \boldsymbol{\mu}) = a_0(\mathbf{x}) + \sum_{i=1}^N a_i(\mathbf{x})\mu_i = a_0(\mathbf{x}) + \sum_{i=1}^N \sqrt{\lambda_i} c_i(\mathbf{x})\mu_i, \quad (5.2)$$

Here, the covariance function of the random field is given by

$$\text{Cov}(\mathbf{x}, \mathbf{y}) = \sigma^2 \exp\left(-\frac{|x_1 - y_1|}{c} - \frac{|x_2 - y_2|}{c}\right).$$

The Gaussian point source at the center of the domain is used as the source term, i.e.,

$$f(\mathbf{x}) = e^{-(8.4)^2((x_1-0.5)^2+(x_2-0.5)^2)}$$

For this test problem, we assume that the random variables  $\{\mu_i\}_{i=1}^N$  are independent and uniformly distributed within the range  $[-1, 1]$ . The parameters of  $a(\mathbf{x}, \boldsymbol{\mu})$  are set as shown in Table 5.4. We use the perfectly matched layers (PML) to simulate the Sommerfeld condition [4], and generate the matrices  $\{\mathbf{A}_i\}_{i=1}^K$  using the codes associated with [13]. The meshgrid in the physical domain is set to  $33 \times 33$  (i.e.,  $n_x = 33$ ), and the total degree of the gPC basis functions in the AASG method is set to  $p = 6$ . The linear systems arising from both the standard stochastic Galerkin method and the AASG method are solved using the preconditioned bi-conjugate gradient stabilized (Bi-CGSTAB) method, with a tolerance of  $10^{-8}$  and the mean based preconditioner [15].

Table 5.4: Parameters of the Helmholtz coefficient  $a(\mathbf{x}, \boldsymbol{\mu})$  in (5.2) and  $K$  in (2.2).

Case	$a_0(\mathbf{x})$	$c$	$\sigma$	$N$	$K$
I	$4 \cdot (2\pi)$	1	$2\pi$	4	25
II	$4 \cdot (2\pi)$	1	$2\pi$	10	121

### 5.2.1 Case I: a 4 dimensional Helmholtz problem

We consider the AASG method with decreasing tolerances  $\text{TOL} = \{10^{-1}, 10^{-2}, 10^{-3}, 10^{-4}, 10^{-5}\}$  to demonstrate its effectiveness and efficiency. To assess the accuracy of the AASG method and the MCM, we obtain the reference solution  $u_{\text{REF}}(\mathbf{x}, \boldsymbol{\mu})$  using the standard stochastic Galerkin method with the total degree of up to  $p = 8$ .

Table 5.5: Performance of the AASG method for different TOL.

TOL	$ \mathfrak{J}_1 $	$ \tilde{\mathfrak{J}}_1 $	$ \mathfrak{J}_2 $	$ \tilde{\mathfrak{J}}_2 $	$ \mathfrak{J}_3 $	$ \tilde{\mathfrak{J}}_3 $	$ \mathfrak{J}_4 $	$ \tilde{\mathfrak{J}}_4 $	$k$	$ \mathfrak{m}_k^{6^\dagger} $	CPU time
$10^{-1}$	4	1	0	0	0	0	0	0	1	25	0.19
$10^{-2}$	4	4	6	3	0	0	0	0	2	115	1.52
$10^{-3}$	4	4	6	5	2	1	0	0	3	155	3.63
$10^{-4}$	4	4	6	6	4	3	0	0	3	195	4.54
$10^{-5}$	4	4	6	6	4	4	1	1	4	210	8.05

Table 5.5 presents the number of active indices for each order of ANOVA decomposition and the total number of selected gPC basis functions in the stochastic space. We also report the computational time required for solving the resulting linear systems using the preconditioned Bi-CGSTAB method with a tolerance of  $10^{-8}$  and the mean based preconditioner. It can be observed that the number of selected gPC basis functions increases as the tolerance TOL decreases. For a 4 dimensional problem, there are  $C_{10}^6 = 210$  gPC basis functions with the total degree up to 6. From the table, it can be seen that when  $\text{TOL} = 10^{-5}$ , all the gPC basis functions are selected in the AASG method, making the AASG method equivalent to the standard stochastic Galerkin method.

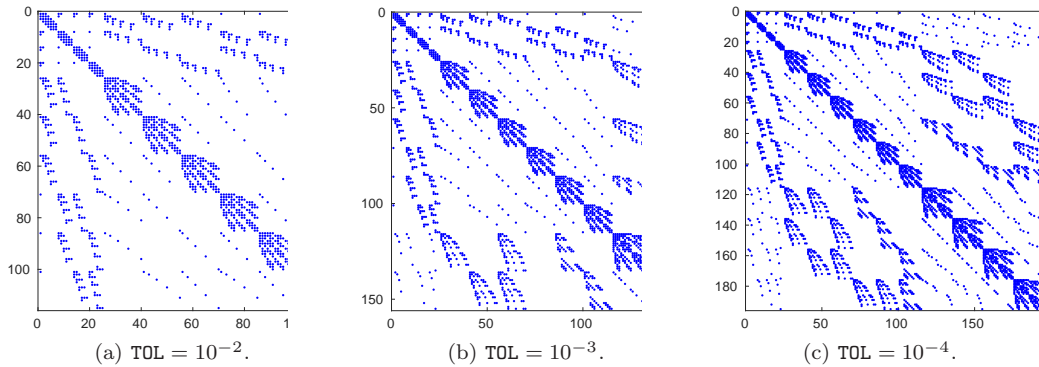


Fig. 5.5: Matrix block-structure (each block has dimension  $n_x \times n_x$ ) for  $\text{TOL} = 10^{-2}, 10^{-3}, 10^{-4}$ .

Figure 5.5 illustrates the block structure of the coefficient matrix of the resulting linear system. Each point in the figure represents a block of dimension  $n_x \times n_x$ . Moreover, each nonzero block of

the coefficient matrix has the same sparsity pattern as the corresponding deterministic problem. Although the coefficient matrix of the Helmholtz equation is much denser than that of the diffusion equation, it is still very sparse and thus should be solved by iterative methods.

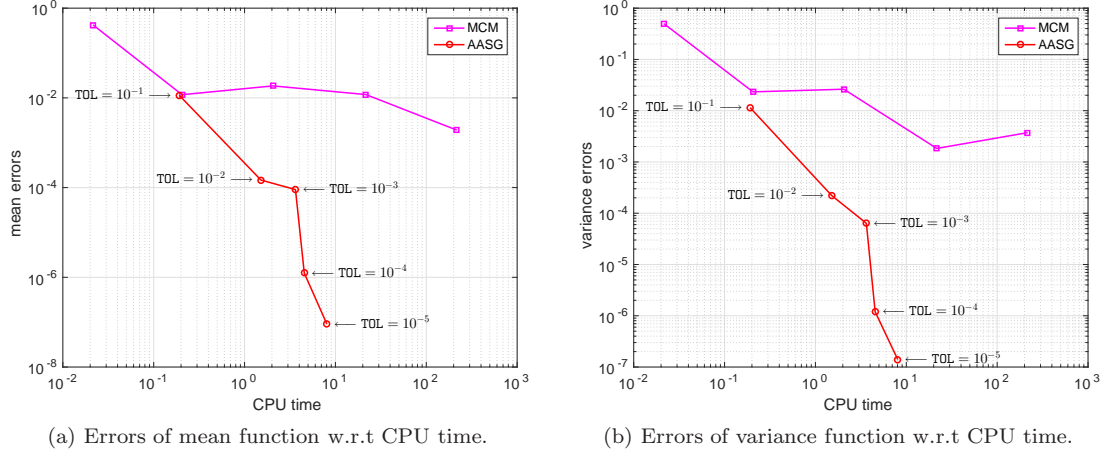


Fig. 5.6: Comparison of CPU time for the MCM and the AASG method.

Figure 5.6 displays the CPU time of the MCM and the AASG method as a function of the mean and the variance errors. The CPU time considered in this problem correspond to the total time of solving the linear systems in the respective procedures. The results indicate that the AASG method is more efficient than MCM. It can be seen that the AASG method with a tolerance of  $\text{TOL} = 10^{-2}$  is more accurate than the MCM with  $10^5$  samples.

### 5.2.2 Case II: a 10 dimensional Helmholtz problem

We consider the AASG method with decreasing tolerances  $\text{TOL} = \{10^{-1}, 10^{-2}, 10^{-3}, 10^{-4}, 10^{-5}\}$  to demonstrate its effectiveness and efficiency. To access the accuracy of the AASG method and the MCM, we obtain the reference solution  $u_{\text{REF}}(\mathbf{x}, \boldsymbol{\mu})$  using the standard stochastic Galerkin method with the total degree of up to  $p = 8$ .

Table 5.6 presents the number of active indices for each order of ANOVA decomposition and the total number of selected gPC basis functions in the stochastic space. We also report the computational time required for solving the resulting linear systems using the preconditioned Bi-CGSTAB method with a tolerance of  $10^{-8}$  and the mean based preconditioner. It can be observed that the number of selected gPC basis functions increases as the tolerance  $\text{TOL}$  decreases, and therefore, the accuracy can be improved by reducing  $\text{TOL}$ .

Figure 5.7 illustrates the block structure of the coefficient matrix of the resulting linear system. Each point in the figure represents a block of dimension  $n_x \times n_x$ . Moreover, each nonzero block of the coefficient matrix has the same sparsity pattern as the corresponding deterministic problem. It can be observed that the coefficient matrix of the Helmholtz equation is much denser than that of the diffusion equation, which makes it more time consuming to solve than the diffusion problem.

Table 5.6: Performance of the AASG method for different TOL.

TOL	$ \tilde{\mathcal{J}}_1 $	$ \tilde{\mathcal{J}}_1 $	$ \tilde{\mathcal{J}}_2 $	$ \tilde{\mathcal{J}}_2 $	$ \tilde{\mathcal{J}}_3 $	$ \tilde{\mathcal{J}}_3 $	$ \tilde{\mathcal{J}}_4 $	$ \tilde{\mathcal{J}}_4 $	$k$	$ m_k^{\phi^\dagger} $	CPU time
$10^{-1}$	10	1	0	0	0	0	0	0	1	61	0.72
$10^{-2}$	10	9	36	6	0	0	0	0	2	601	14.10
$10^{-3}$	10	10	45	14	7	3	0	0	3	876	41.32
$10^{-4}$	10	10	45	32	55	21	0	0	3	1836	76.56
$10^{-5}$	10	10	45	43	105	59	41	22	4	3451	269.12

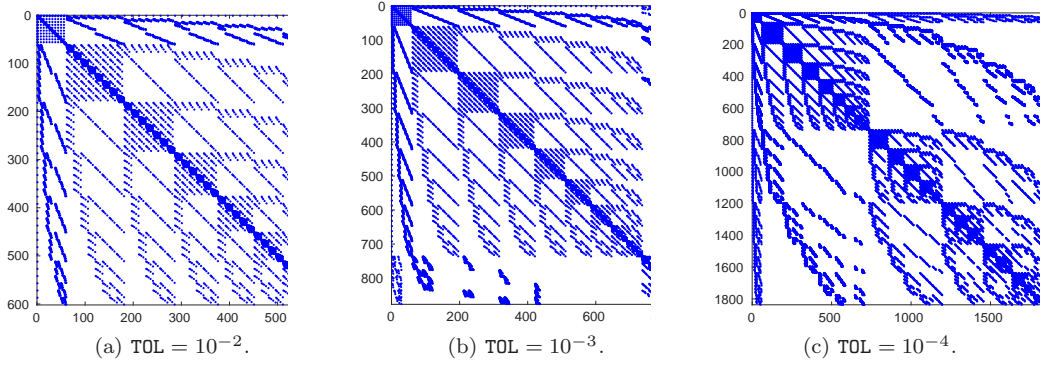


Fig. 5.7: Matrix block-structure (each block has dimension  $n_x \times n_x$ ) for TOL =  $10^{-2}, 10^{-3}, 10^{-4}$ .

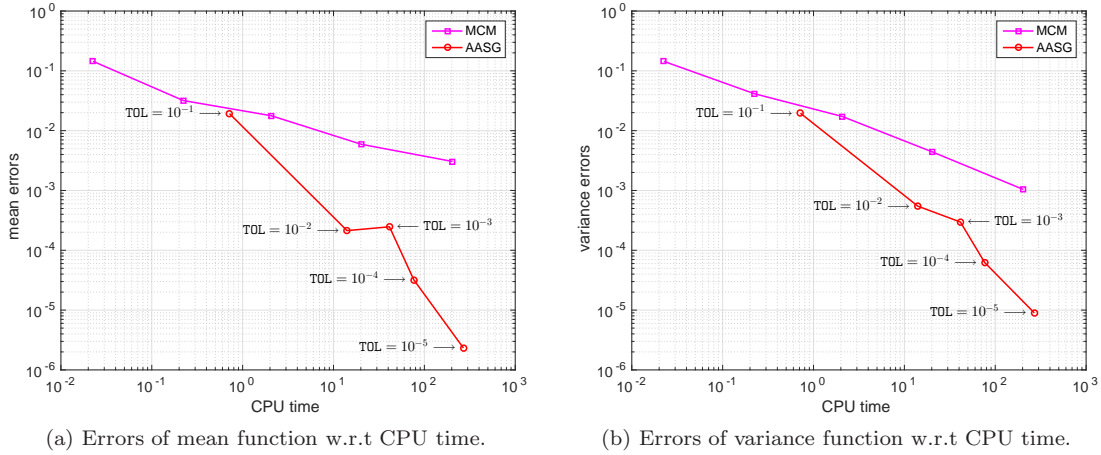


Fig. 5.8: Comparison of CPU time for the MCM and the AASG method.

Figure 5.8 displays the CPU time of the MCM and the AASG method as a function of the mean and the variance errors. The results clearly indicate that the AASG method outperforms MCM in terms of efficiency. Specifically, we observe that the AASG method achieves a level of accuracy comparable to that of MCM with  $10^5$  samples, when a tolerance of  $\text{TOL} = 10^{-2}$  is used.

## 6 Conclusion

In this work, we investigate the generalized polynomial chaos (gPC) expansion of component functions for the ANOVA decomposition, and present a concise form of the gPC expansion for each component function. With this foundation, we propose an adaptive ANOVA stochastic Galerkin method for solving partial differential equations with random inputs. The proposed method effectively selects basis functions in the stochastic space, enabling significant reduction in the dimension of the stochastic approximation space. Numerical simulations are conducted to demonstrate the effectiveness and efficiency of the proposed method. While our current focus is on selecting the basis in the stochastic space, future work will explore techniques for reducing computational costs in the physical space.

## References

1. Agarwal, N., Aluru, N.R.: A domain adaptive stochastic collocation approach for analysis of MEMS under uncertainties. *Journal of Computational Physics* **228**(20), 7662–7688 (2009). DOI 10.1016/j.jcp.2009.07.014
2. Askey, R.: *Orthogonal polynomials and special functions*. SIAM (1975)
3. Babuška, I., Tempone, R.L., Zouraris, G.E.: Galerkin finite element approximations of stochastic elliptic partial differential equations. *SIAM Journal on Numerical Analysis* **42**(2), 800–825 (2004). DOI 10.1137/S0036142902418680
4. Berenger, J.P.: A perfectly matched layer for the absorption of electromagnetic waves. *Journal of Computational Physics* **114**(2), 185–200 (1994). DOI 10.1006/jcph.1994.1159
5. Cafisch, R.E.: Monte Carlo and quasi-Monte Carlo methods. *Acta numerica* **7**, 1–49 (1998)
6. Elman, H., Furnival, D.: Solving the stochastic steady-state diffusion problem using multigrid. *IMA Journal of Numerical Analysis* **27**(4), 675–688 (2007). DOI 10.1093/imanum/drm006
7. Elman, H.C., Ernst, O.G., O’Leary, D.P., Stewart, M.: Efficient iterative algorithms for the stochastic finite element method with application to acoustic scattering. *Computer Methods in Applied Mechanics and Engineering* **194**, 1037–1055 (2005). DOI 10.1016/j.cma.2004.06.028
8. Feng, X., Lin, J., Lorton, C.: An efficient numerical method for acoustic wave scattering in random media. *SIAM/ASA Journal on Uncertainty Quantification* **3**(1), 790–822 (2015). DOI 10.1137/140958232
9. Fishman, G.: *Monte Carlo: concepts, algorithms, and applications*. Springer Science & Business Media (2013)
10. Gao, Z., Hesthaven, J.S.: On ANOVA expansions and strategies for choosing the anchor point. *Applied Mathematics and Computation* **217**(7), 3274–3285 (2010). DOI 10.1016/j.amc.2010.08.061
11. Ghanem, R.G., Spanos, P.D.: *Stochastic finite elements: a spectral approach*. Courier Corporation (2003)
12. Liao, Q., Lin, G.: Reduced basis ANOVA methods for partial differential equations with high-dimensional random inputs. *Journal of Computational Physics* **317**, 148–164 (2016). DOI 10.1016/j.jcp.2016.04.029
13. Liu, F., Ying, L.: Additive sweeping preconditioner for the Helmholtz equation. *Multiscale Modeling & Simulation* **14**(2), 799–822 (2016). DOI 10.1137/15M1017144
14. Ma, X., Zabaras, N.: An adaptive high-dimensional stochastic model representation technique for the solution of stochastic partial differential equations. *Journal of Computational Physics* **229**(10), 3884–3915 (2010). DOI 10.1016/j.jcp.2010.01.033
15. Powell, C.E., Elman, H.C.: Block-diagonal preconditioning for spectral stochastic finite element systems. *IMA Journal of Numerical Analysis* **29**(2), 350–375 (2009). DOI 10.1093/imanum/drn014
16. Sobol’, I.M.: Theorems and examples on high dimensional model representation. *Reliability Engineering and System Safety* **79**(2), 187–193 (2003). DOI 10.1016/S0951-8320(02)00229-6
17. Sudret, B.: Global sensitivity analysis using polynomial chaos expansions. *Reliability engineering & system safety* **93**(7), 964–979 (2008). DOI 10.1016/j.res.2007.04.002

18. Tang, K., Congedo, P.M., Abgrall, R.: Sensitivity analysis using anchored ANOVA expansion and high-order moments computation. *International Journal for Numerical Methods in Engineering* **102**(9), 1554–1584 (2015). DOI 10.1002/nme.4856
19. Tang, K., Congedo, P.M., Abgrall, R.: Adaptive surrogate modeling by ANOVA and sparse polynomial dimensional decomposition for global sensitivity analysis in fluid simulation. *Journal of Computational Physics* **314**(1), 557–589 (2016). DOI 10.1016/j.jcp.2016.03.026
20. Wan, X., Karniadakis, G.E.: An adaptive multi-element generalized polynomial chaos method for stochastic differential equations. *Journal of Computational Physics* **209**(2), 617–642 (2005). DOI 10.1016/j.jcp.2005.03.023
21. Wang, X.: On the approximation error in high dimensional model representation. In: 2008 Winter Simulation Conference, pp. 453–462. IEEE (2008). DOI 10.1109/WSC.2008.4736100
22. Xiu, D.: Numerical methods for stochastic computations: a spectral method approach. Princeton University Press (2010)
23. Xiu, D., Hesthaven, J.: High-order collocation methods for differential equations with random inputs. *SIAM Journal on Scientific Computing* **27**, 1118–1139 (2005). DOI 10.1137/040615201
24. Xiu, D., Karniadakis, G.E.: Modeling uncertainty in steady state diffusion problems via generalized polynomial chaos. *Computer Methods in Applied Mechanics and Engineering* **191**(43), 4927–4948 (2002). DOI 10.1016/S0045-7825(02)00421-8
25. Xiu, D., Karniadakis, G.E.: The Wiener-Askey polynomial chaos for stochastic differential equations. *SIAM journal on scientific computing* **24**(2), 619–644 (2002). DOI 10.1137/S1064827501387826
26. Xiu, D., Karniadakis, G.E.: Modeling uncertainty in flow simulations via generalized polynomial chaos. *Journal of computational physics* **187**(1), 137–167 (2003). DOI doi:10.1016/S0021-9991(03)00092-5
27. Yang, X., Choi, M., Lin, G., Karniadakis, G.E.: Adaptive ANOVA decomposition of stochastic incompressible and compressible flows. *Journal of Computational Physics* **231**(4), 1587–1614 (2012)